# LINEAR FEEDBACK CONTROL FOR A NONLINEAR MULTIROTOR AERIAL VEHICLE MODEL WITH STOCHASTIC PARAMETER UNCERTAINTIES

**Mateus de Freitas Virgílio Pereira, mateusfvp@hotmail.com**[1]
**Davi Ferreira de Castro, davifc@ita.br**[1]
**Igor Afonso Acampora Prado, igorap@ita.br**[1]
**Davi Antônio dos Santos, davists@ita.br**[1]
**José Manoel Balthazar, jmbaltha@ita.br**[1]

[1]Aeronautics Institute of Technology (ITA), Praça Marechal Eduardo Gomes, 50 - Vila das Acácias, São José dos Campos - SP, 12228-900, Brazil.

***Abstract:*** *In this paper, we present a polynomial chaos-based framework for designing optimal linear feedback control laws for a nonlinear multirotor aerial vehicle model with stochastic parameter uncertainty. The spectral decomposition in orthogonal polynomial basis, prescribed by the Wiener-Askey scheme, provides a deterministic framework from which the control design is derived. Optimality of the proposed control law is proved by solving the Hamilton-Jacobi-Bellman equation and asymptotically stability of the controlled nonlinear systems is guaranteed in the Lyapunov sense. Numerical simulations were carried out for a quadrotor model that accounts for the coupling between the dynamical modes. The results are verified with Monte-Carlo simulations.*
***Keywords:*** *Polynomial chaos, Uncertainty, Multirotor aerial vehicles, Linear feedback control.*

## 1. INTRODUCTION

Multirotor Aerial Vehicles (MAVs) have motivated many researches in different fields of knowledge such as sensors fusion (Cheviron *et al.* (2007)), computer vision (Saripalli *et al.* (2003)) and control strategies (Santos *et al.* (2013)). Although there is a massive amount of concluded and ongoing research works on MAVs, the design of control laws for such vehicles still has challenges to be overcome. In real implementations, such control systems ought to be robust, that is, capable of working properly, within the designed specifications, even when subject to either disturbances or uncertainties in the determination of the system parameters.

The control of MAVs with unknown parameters or operating in uncertain environments has been an important topic of research. For instance, Raffo *et al.* (2010) designs a nonlinear $H_\infty$ controller to stabilize the rotational movements of a MAV model with uncertain parameters subjected to a constant disturbance. Bialy *et al.* (2013) develops a robust adaptive controller for the dynamics of a quadrotor with unknown parameters and bounded exogenous perturbations.Kada and Ghazzawi (2011) presents a design scheme that combines deadbeat response, robust control, and model reduction techniques to enhance the performances and robustness of PID controller for a unmanned vehicle.

The Linear Quadratic Regulator (LQR) is an usual control strategy applied to MAVs (Bouabdallah *et al.* (2004)), which requires a linear design model. Such linear model does not take into account the nonlinear phenomena that are present in the real operation of these vehicles. However, for a more effective control law, nonlinearities have to be considered in order to avoid unstable regions of operation. Rafikov and Balthazar (2008) and Rafikov *et al.* (2008) introduced an optimal linear feedback to handle the task of controlling nonlinear dynamical systems. Asymptotic stability of the closed-loop nonlinear system was proved by selecting a Lyapunov function, which could be seen to be the solution of the Hamilton-Jacobi-Bellman equation thus guaranteeing both stability and optimality. Due to the simple configuration and easy implementation, the use of linear control is preferred over the nonlinear design. Pereira *et al.* (2016) (to appear) extended the work of Rafikov and Balthazar to nonlinear systems with stochastic parameter uncertainty by implementing a polynomial-chaos based framework to design stochastic optimal linear control policies.

Polynomial chaos expansion is an alternative to sampling methods, since it provides a simpler framework to deal with the propagation of uncertainty in the dynamical model. It is the spectral decomposition of a stochastic process in the random dimension in which it is parametrized. The random trial basis is the Askey-scheme based orthogonal polynomials. Introduced first by Wiener (1938) for Gaussian random variables and then generalized by Xiu and Karniadakis (2002) for other probability distributions, such decomposition is based on the Cameron-Martin Theorem (Cameron and Martin (1947)), which guarantees the convergence in $L^2$ sense for stochastic processes with finite second moment. Many researches have attested that spectral methods based on polynomial chaos expansions can be a computationally efficient alternative to expensive conventional approaches based on Monte Carlo sampling (Xiu and Karniadakis (2002); Fisher and Bhattacharya (2009); Prabhakar *et al.* (2010); Xiu and Karniadakis (2003)).

The use of polynomial chaos expansions in control theory is recent. Hover and Triantafyllou (2006) demonstrated that this method applies to the stability study of nonlinear systems, especially when the methods of Lyapunov are inconclusive and Monte Carlo simulations are expensive. Fisher and Bhattacharya (2009, 2006, 2008) presented a generalized procedure for the stability analysis of linear and polynomial systems and a systematic framework for designing linear quadratic regulators (LQR) for stochastic linear systems using polynomial chaos expansions. The work of Pereira *et al.* (2016) (to appear)follows a similar approach to design a LQR-like control for nonlinear systems with uncertain parameters.

This work applies the polynomial chaos expansions for designing a linear feedback control for a nonlinear quadrotor model with stochastic parameter uncertainties. Random disturbances from an uncertain environment are also considered. We use the polynomial chaos expansion to propagate uncertainties trhough the MAV model and to create a deterministic framework from which the control design is derived.

This paper is organized as follows. We first present the quadrotor dynamical model. Next we present the polynomial chaos expansion and the Wiener-Askey scheme, and apply the spectral decomposition to transform the MAV stochastic nonlinear dynamics into a higher dimension deterministic system, which is used to derive the optimal linear feedback control law. The proposed method is validated by numerical simulations of the MAV subjected to random disturbances. The results are then verified with the traditional Monte Carlo simulations in the statistical sense.

## 2. MULTIROTOR AERIAL VEHICLE MODEL

This section presents the equations of motion of a multirotor aerial vehicle (MAV), considering all the relevant effects necessary to be accounted for in ground-thruth model for simulation-based evaluation of control laws.

### 2.1 Preliminary definitions

We define two Cartesian coordinate systems (CCS) as illustrated in Fig. 1. The body CCS, $S_{\mathrm{B}} \triangleq \{X_{\mathrm{B}}, Y_{\mathrm{B}}, Z_{\mathrm{B}}\}$ is attached to the vehicle's body with the origin at the vehicle's center of mass (CM), the $X_{\mathrm{B}}$ axis pointing forward, the $Z_{\mathrm{B}}$ axis pointing upward, perpendicular to the plane of the rotors, and the $Y_{\mathrm{B}}$ axis completing a dextrogeous frame. The CCS, $S_{\mathrm{G}} = \{X_{\mathrm{G}}, Y_{\mathrm{G}}, Z_{\mathrm{G}}\}$ is fixed to the ground at a known point $O$, with the $Z_{\mathrm{G}}$ axis pointing upward, aligned with the local vertical.

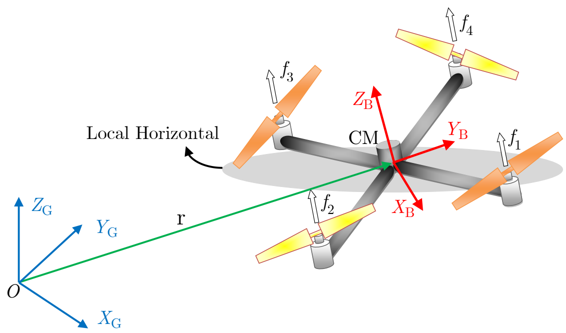


Figure 1: **The Cartesian coordinate systems (CCS).** $S_{\mathrm{B}} = \{X_{\mathrm{B}}, Y_{\mathrm{B}}, Z_{\mathrm{B}}\}$ **is the body CCS and** $S_{\mathrm{G}} = \{X_{\mathrm{G}}, Y_{\mathrm{G}}, Z_{\mathrm{G}}\}$ **is the ground CCS.**

### 2.2 Resultant control thrust and torque

We consider a quadrotor configuration with the longitudinal axis $X_{\mathrm{B}}$ pointing between rotor 1 and rotor 2, and with 45 degree of separation angle between adjacent arms; we call it the "x" configuration. Moreover, we consider that rotor 1 and rotor 3 rotate in clockwise direction, while rotor 2 and rotor 4 rotate in counterclockwise direction. For the aforementioned configuration, one can show that the relationship between the individual rotor thrusts $f_i$ and the resultant thrust magnitude and torque vector is given by

$$\begin{bmatrix} F^c \\ \mathbf{T}^c \end{bmatrix} = \mathbf{\Gamma}\mathbf{f}, \tag{1}$$

with $\mathbf{f} \triangleq \begin{bmatrix} f_1 & f_2 & f_3 & f_4 \end{bmatrix}^{\mathrm{T}}$ and

$$\mathbf{\Gamma} \triangleq \begin{bmatrix} 1 & 1 & 1 & 1 \\ l/\sqrt{2} & -l/\sqrt{2} & -l/\sqrt{2} & l/\sqrt{2} \\ -l/\sqrt{2} & -l/\sqrt{2} & l/\sqrt{2} & l/\sqrt{2} \\ k_\tau/k_f & -k_\tau/k_f & k_\tau/k_f & -k_\tau/k_f \end{bmatrix}, \tag{2}$$

where $l$ is the length of each vehicle's arm. The superscript $c$ in Eq. (1) stands for the control command defined by the operator and is used to distinguish from the other sources of force and torque that will be presented soon.

By inverting Eq. (2), one can compute the command $\bar{\mathbf{f}} \triangleq \begin{bmatrix} \bar{f}_1 & \bar{f}_2 & \bar{f}_3 & \bar{f}_4 \end{bmatrix}^{\mathrm{T}}$ as

$$\bar{\mathbf{f}} = \Xi \begin{bmatrix} \bar{F}^c \\ \bar{\mathbf{T}}^c \end{bmatrix}, \tag{3}$$

where $\Xi \triangleq \Gamma^{-1}$, $\bar{F}^c$ is the thrust magnitude command, and $\bar{\mathbf{T}}^c$ is the control torque command. Note that the rotor dynamics is not considered here, since we suppose that the motor response is imeadiate to the command input.

### 2.3 Rotational motion

Representing the attitude using the Euler angles $\boldsymbol{a}_\alpha \triangleq \begin{bmatrix} \phi & \theta & \psi \end{bmatrix}^{\mathrm{T}}$ in the rotation sequence 1-2-3, we have the following rotational kinematics equations:

$$\dot{\boldsymbol{a}_{\boldsymbol{\alpha}}} = \mathcal{A}\mathbf{\Omega} \tag{4}$$

where $\mathbf{\Omega} \triangleq [\Omega_x \ \Omega_y \ \Omega_z]^{\mathrm{T}}$ is the $S_{\mathrm{B}}$ representation of the vehicle's angular velocity w.r.t. $S_{\mathrm{G}}$ and

$$\mathcal{A} \triangleq \begin{bmatrix} \cos\psi/\cos\theta & -\sin\phi/\cos\theta & 0 \\ \sin\psi & \cos\psi & 0 \\ -\cos\psi\sin\theta/\cos\theta & \sin\psi\sin\theta/\cos\theta & 1 \end{bmatrix} \tag{5}$$

Assume that the vechile has a rigid structure and $S_{\mathrm{G}}$ is an inertial frame. Considering the existence of gyroscopic effects, due to the rotors, and disturbance torques, and using the Newton-Euler formulation, one can model the rotational dynamics of the MAV by

$$\dot{\mathbf{\Omega}} = \mathbf{J}^{-1}(\mathbf{J}\mathbf{\Omega}) \times \mathbf{\Omega} + I_r\mathbf{J}^{-1}\mathbf{\Omega} \times \mathbf{e}_3 \sum_{i=1}^{4} (-1)^i \omega_i + \mathbf{J}^{-1}\mathbf{T}^c + \mathbf{J}^{-1}\mathbf{T}^d \tag{6}$$

where $\mathbf{T}^c$ and $\mathbf{T}^d$ are the $S_{\mathrm{B}}$ representations of the resultant control torque and disturbance torque, respectively, $\mathbf{e}_3 \triangleq [0 \ \ 0 \ \ 1]^{\mathrm{T}}$, $I_r$ is the moment of inertia of the rotors w.r.t. the rotation axis, and $\mathbf{J}$ is the body inertia matrix. Consider that the vehicle has a symmetric structure with known mass $m$ and inertia matrix in $S_{\mathrm{B}}$

$$\mathbf{J} = \begin{bmatrix} J_x & 0 & 0 \\ 0 & J_y & 0 \\ 0 & 0 & J_z \end{bmatrix}. \tag{7}$$

The second term in the right-hand side of Eq. (6) corresponds to the gyroscopic moment due to the rotor dynamics and it has little effects on the vehicle dynamics and therefore will be neglected (Prado and Santos (2014)). Hence, the state-space model for rotation can be represented as:

$$\dot{\mathbf{x}}(t) = \mathbf{A}\mathbf{x}(t) + \mathbf{h}(\mathbf{x}) + \mathbf{B}\mathbf{u}(t) \tag{8}$$

where

$$\mathbf{x} \triangleq \begin{bmatrix} \phi & \theta & \psi & \Omega_x & \Omega_y & \Omega_z \end{bmatrix}^{\mathrm{T}} \in \mathbb{R}^6, \tag{9}$$

$$\mathbf{u} \triangleq \mathbf{T}^c \in \mathbb{R}^3, \tag{10}$$

and

$$\mathbf{A} = \begin{bmatrix} 0 & 0 & 0 & 1 & 0 & 0 \\ 0 & 0 & 0 & 0 & 1 & 0 \\ 0 & 0 & 0 & 0 & 0 & 1 \\ 0 & 0 & 0 & 0 & 0 & 0 \\ 0 & 0 & 0 & 0 & 0 & 0 \\ 0 & 0 & 0 & 0 & 0 & 0 \end{bmatrix} \quad \mathbf{B} = \begin{bmatrix} 0 & 0 & 0 \\ 0 & 0 & 0 \\ 0 & 0 & 0 \\ \frac{1}{J_x} & 0 & 0 \\ 0 & \frac{1}{J_y} & 0 \\ 0 & 0 & \frac{1}{J_z} \end{bmatrix} \quad \mathbf{h}(\mathbf{x}) = \begin{bmatrix} -\Omega_x + \Omega_x \frac{\cos\psi}{\cos\theta} - \Omega_y \frac{\sin\psi}{\cos\theta} \\ -\Omega_y + \Omega_x \sin\psi + \Omega_y \cos\psi \\ \Omega_z - \Omega_x \frac{\cos\psi\sin\theta}{\cos\theta} + \Omega_y \frac{\sin\psi\sin\theta}{\cos\theta} \\ \frac{(J_y - J_z)}{J_x}\Omega_y\Omega_z \\ \frac{(J_z - J_x)}{J_y}\Omega_x\Omega_z \\ \frac{(J_x - J_y)}{J_z}\Omega_x\Omega_y \end{bmatrix} \tag{11}$$

## 3. POLYNOMIAL CHAOS EXPANSION

In this section we introduce the polynomial chaos expansion for representing a stochastic process according to the Wiener's theory of homogeneous chaos (Wiener (1938)). We also describe the use of such framework to transform stochastic nonlinear dynamical systems into an augmented deterministic system for the decomposition coefficients.

### 3.1 The Wiener-Askey Scheme

Define the set of multi-indices with finite number of nonzero components as

$$\mathcal{J} = \left\{ \boldsymbol{\alpha} = (\alpha_i)_{i\geq 1}, \alpha_i \in \mathbb{N}, |\boldsymbol{\alpha}| = \sum_{i=1}^{\infty} \alpha_i < \infty \right\}. \tag{12}$$

For an index $\boldsymbol{\alpha} \in \mathcal{J}$, the Wick polynomial of order $|\boldsymbol{\alpha}|$ in an infinite number of independent and identically distributed normal random variables $\boldsymbol{\xi} = (\xi_1, \xi_2, \ldots)$ is defined by

$$\Psi_{\boldsymbol{\alpha}}(\boldsymbol{\xi}) = \prod_{i=0}^{\infty} H_{\alpha_i}(\xi_i) \tag{13}$$

where $H_n(\cdot)$ is the normalized $n$-th order multivariate orthogonal Hermite polynomial. The random functions $\Psi_{\boldsymbol{\alpha}}$ form a complete orthonormal basis in $L^2$ on the probability space with respect to the Gaussian measure generated by $\xi$ (Branicki and Majda (2012)). According to the Cameron-Martin theorem (Cameron and Martin (1947)), a finite-variance random variable $g(t, \boldsymbol{\xi})$, where $t$ denotes any deterministic parameter (e.g. the time instant), has the following decomposition in Wick polynomials:

$$g(t, \boldsymbol{\xi}) = \sum_{\boldsymbol{\alpha} \in \mathcal{J}} g_{\boldsymbol{\alpha}}(t) \Psi_{\boldsymbol{\alpha}}(\boldsymbol{\xi}) \tag{14}$$

where $g_{\boldsymbol{\alpha}}(t)$ are the mode strengths given by

$$g_{\boldsymbol{\alpha}}(t) = \frac{\langle g(t, \boldsymbol{\xi}), \Psi_{\boldsymbol{\alpha}}(\boldsymbol{\xi}) \rangle}{\langle \Psi^2_{\boldsymbol{\alpha}}(\boldsymbol{\xi}) \rangle}. \tag{15}$$

Notation $\langle \cdot \rangle$ represents the multivariate inner product in $L^2(D_\xi)$ space and $D_\xi$ is the domain of $\boldsymbol{\xi}$. The spectral expansion in Eq. (14) is referred to as the Polynomial Chaos Expansion (PCE) of the variable $g$. A fundamental property of this expansion is that it converges in the $L^2$ sense. In practice, the PCE will be truncated to a finite number of terms by limiting the germ $\boldsymbol{\xi}$ to $r$ normal random variables and the order of the multivariate polynomials $\Psi_{\boldsymbol{\alpha}}$ to $|\boldsymbol{\alpha}| \leq d$. The resulting number of terms in the truncated expansion is given by $P = \frac{(r+d)!}{r!d!} - 1$ The parameter $P$ has to be chosen large enough for the approximation of Eq. (14) to be accurate.

An interesting result of the expansion presented in Eq. (14) is that the first two statistical moments of the random variable $g$ are readily computed from the terms of the PCE, with no need of Monte Carlo sampling methods. Considering the truncated decomposition, we have:

$$E[g(t, \boldsymbol{\xi})] = E\left[\sum_{k=0}^{P} g_k \Psi_k(\boldsymbol{\xi})\right] = g_0, \tag{16}$$

$$V[g(t, \boldsymbol{\xi})] = V\left[\sum_{k=0}^{P} g_k \Psi_k(\boldsymbol{\xi})\right] = \sum_{k=0}^{P} g_k^2(t) V[\Psi_k(\boldsymbol{\xi})]. \tag{17}$$

Xiu and Karniadakis (2002) extended the PCE framework to non-Gaussian random inputs by elaborating a tree that maps a certain distribution to the corresponding orthogonal polynomial that guarantees the optimal convergence of the expansion. Table 1 shows the pairing for continuous distributed random variables. This broad framework is called Generalized Polynomial Chaos (gPC) expansion and it associates the probability density function of the germ $\boldsymbol{\xi}$ with polynomials within the Askey-scheme that have a similar weight function. Such polynomials form a complete basis in the Hilbert space determined by their corresponding support (Fisher and Bhattacharya (2009); Askey and Wilson (1985)).

The gPC method is especially useful in solving or analyzing stochastic differential equations. In control theory, the use of conventional methods to study the stability and to design a robust controller subject to random inputs can lead inconclusive results or does not cover all the possible scenarios in an efficient way. In this sense, the gPC is a powerful tool since the stability characteristic of a dynamical system can be inferred from the decay of the modes strengths over time (Fisher and Bhattacharya (2006); Hover and Triantafyllou (2006)), that is, in a deterministic framework.

Table 1: **The Wiener-Askey scheme.**

| Random variable $\xi$ | Polynomial basis $\Psi_k$ | Support |
|---|---|---|
| Gaussian | Hermite | $(-\infty, \infty)$ |
| Uniform | Legendre | $[a, b]$ |
| Gamma | Laguerre | $[0, \infty)$ |
| Beta | Jacobi | $[a, b]$ |

### 3.2 Expansion of Stochastic Differential Nonlinear Equations

Consider the following stochastic nonlinear dynamical system:

$$\dot{\boldsymbol{x}}(t, \boldsymbol{\xi}) = \boldsymbol{A}(\boldsymbol{\xi})\boldsymbol{x}(t, \boldsymbol{\xi}) + \boldsymbol{h}(\boldsymbol{x}, \boldsymbol{\xi}) + \boldsymbol{B}(\boldsymbol{\xi})\boldsymbol{u}(t, \boldsymbol{\xi}), \tag{18}$$

where $\boldsymbol{x} \in \mathbf{R}^n$ is the state vector, $\boldsymbol{u} \in \mathbf{R}^m$ is the control input, $\boldsymbol{A} \in \mathbf{R}^{n\times n}$ and $\boldsymbol{B} \in \mathbf{R}^{n\times m}$ are matrices and $\boldsymbol{h} \in \mathbf{R}^n$ is a vector whose components are continuous nonlinear function of $\boldsymbol{x}$. The random variable $\boldsymbol{\xi} = (\xi_1, \xi_2, \ldots, \xi_r)$ represents uncertainties, with a known stationary distribution, by which the parameters of the model or the initial conditions are expressed. The initial state vector is $\boldsymbol{x}(t_0) = \boldsymbol{x}_0(\boldsymbol{\xi})$. Due to the randomness of the system parameters, one can see that the state trajectories will also be stochastic. Here we assume that the control input is computed by some state feedback strategy and therefore will also present a stochastic behavior.

Denote the components of $\boldsymbol{x}(t, \boldsymbol{\xi})$, $\boldsymbol{u}(t, \boldsymbol{\xi})$ and $\boldsymbol{h}(\boldsymbol{x}, \boldsymbol{\xi})$ by, respectively, $x_i(t, \boldsymbol{\xi})$, $u_i(t, \boldsymbol{\xi})$ and $h_i(\boldsymbol{x}, \boldsymbol{\xi})$. Also, denote the elements of $\boldsymbol{A}(\boldsymbol{\xi})$ and $\boldsymbol{B}(\boldsymbol{\xi})$ by, respectively, $A_{ij}(\boldsymbol{\xi})$ and $B_{ij}(\boldsymbol{\xi})$. We can represent $x_i(t, \boldsymbol{\xi})$, $u_i(t, \boldsymbol{\xi})$, $A_{ij}(\boldsymbol{\xi})$, $B_{ij}(\boldsymbol{\xi})$ and $h_i(\boldsymbol{x}, \boldsymbol{\xi})$ by means of the gPC expansion of order $P$ in the orthogonal polynomial basis $\Psi_k(\boldsymbol{\xi})$ according to the Wiener-Askey scheme (see Table 1):

$$x_i(t, \boldsymbol{\xi}) \approx \sum_{k=0}^{P} x_{i,k}(t)\Psi_k(\boldsymbol{\xi}) \tag{19}$$

$$u_i(t, \boldsymbol{\xi}) \approx \sum_{k=0}^{P} u_{i,k}(t)\Psi_k(\boldsymbol{\xi}) \tag{20}$$

$$A_{ij}(\boldsymbol{\xi}) \approx \sum_{k=0}^{P} a_{ij,k}\Psi_k(\boldsymbol{\xi}) \tag{21}$$

$$B_{ij}(\boldsymbol{\xi}) \approx \sum_{k=0}^{P} b_{ij,k}\Psi_k(\boldsymbol{\xi}) \tag{22}$$

$$h_i(\boldsymbol{x}, \boldsymbol{\xi}) \approx \sum_{k=0}^{P} h_{i,k}\Psi_k(\boldsymbol{\xi}) \tag{23}$$

Note that, as long as the relation between $\boldsymbol{h}$ and $\boldsymbol{x}$ is known, the expansion for $h_i(\boldsymbol{x}, \boldsymbol{\xi})$, Eq. (23), may be reformulated in terms of the expansions $x_i(t, \boldsymbol{\xi})$ (see Section 3.2.2).

Let us define the following vector notation for the mode strengths appearing in Eq. (19)-(23):

$$\boldsymbol{x}_i \triangleq \begin{bmatrix} x_{i,0}(t) & x_{i,1}(t) & \ldots & x_{i,P}(t) \end{bmatrix}^T \in \mathbb{R}^{P+1}, \tag{24}$$

$$\boldsymbol{u}_i \triangleq \begin{bmatrix} u_{i,0}(t) & u_{i,1}(t) & \ldots & u_{i,P}(t) \end{bmatrix}^T \in \mathbb{R}^{P+1}, \tag{25}$$

Define also the matrices $\boldsymbol{A}_k \in \mathbb{R}^{(n\times n)}$ with $\{A_k\}_{ij} = a_{ij,k}(t)$ and $\boldsymbol{B}_k \in \mathbb{R}^{(n\times m)}$ with $\{B_k\}_{ij} = b_{ij,k}$ for $k = 0, \ldots, P$. Using the intrusive approach in Xiu and Karniadakis (2002), the coefficients $a_{ij,k}(t)$ and $b_{ij,k}$ are computed by the Galerkin projection of each mode onto the polynomial basis $\{\Psi_q\}_{q=0}^{P}$, in order to ensure the error is orthogonal to the functional space spanned by the finite-dimensional basis $\Psi_k$:

$$a_{ij,k} = \frac{\langle A_{ij}(\boldsymbol{\xi}), \Psi_k(\boldsymbol{\xi})\rangle}{\langle \Psi_k^2(\boldsymbol{\xi})\rangle}, \tag{26}$$

$$b_{ij,k} = \frac{\langle B_{ij}(\boldsymbol{\xi}), \Psi_k(\boldsymbol{\xi})\rangle}{\langle \Psi_k^2(\boldsymbol{\xi})\rangle}. \tag{27}$$

The modes strengths $\boldsymbol{x}_i$, $\boldsymbol{u}_i$ and $\boldsymbol{h}_i$ are also worked out in an intrusive way by employing the Galerkin projection. The gPC expansions from Eq. (19) to (23) are substituted into the original system, Eq. (18), and the projection with respect to the polynomial basis is taken, yielding a system of $n(P+1)$ deterministic ordinary differential equations for the modes. The derivation of such system can be performed in two steps: one for the linear part and the other for the nonlinear part.

#### 3.2.1 Linear Part

Consider the linear part of Eq. (18), that is, $\dot{\boldsymbol{x}} = \boldsymbol{A}\boldsymbol{x} + \boldsymbol{B}\boldsymbol{u}$. The gPC expansion and subsequent Galerkin projection onto $\{\Psi_q\}_{q=0}^{P}$ result in(Fisher and Bhattacharya (2009, 2006, 2008)):

$$\dot{\boldsymbol{\mathcal{X}}} = \boldsymbol{\mathcal{A}}\boldsymbol{\mathcal{X}} + \boldsymbol{\mathcal{B}}\boldsymbol{\mathcal{U}} \tag{28}$$

where $\boldsymbol{\mathcal{X}} \in \mathbb{R}^{n(P+1)}$ and $\boldsymbol{\mathcal{U}} \in \mathbb{R}^{m(P+1)}$ are given by

$$\boldsymbol{\mathcal{X}} = \left[\begin{array}{cccc} \boldsymbol{x}_1^T & \boldsymbol{x}_2^T & \dots & \boldsymbol{x}_n^T \end{array}\right]^T, \tag{29}$$

$$\boldsymbol{\mathcal{U}} = \left[\begin{array}{cccc} \boldsymbol{u}_1^T & \boldsymbol{u}_2^T & \dots & \boldsymbol{u}_m^T \end{array}\right]^T. \tag{30}$$

Matrices $\boldsymbol{\mathcal{A}} \in \mathbb{R}^{n(P+1)\times n(P+1)}$ and $\boldsymbol{\mathcal{B}} \in \mathbb{R}^{n(P+1)\times m(P+1)}$ are defined as:

$$\boldsymbol{\mathcal{A}} = \sum_{k=0}^{P} \boldsymbol{A}_k \otimes \boldsymbol{E}_k \tag{31}$$

$$\boldsymbol{\mathcal{B}} = \sum_{k=0}^{P} \boldsymbol{B}_k \otimes \boldsymbol{E}_k \tag{32}$$

where $\boldsymbol{A}_k$ and $\boldsymbol{B}_k$ are defined below Eq. (25), $\otimes$ denotes the Kronecker product and $\boldsymbol{E}_k \in \mathbb{R}^{(P+1)\times(P+1)}$ is a symmetric matrix given by:

$$\boldsymbol{E}_k = \left[\begin{array}{cccc} \hat{e}_{1k1} & \hat{e}_{1k2} & \dots \hat{e}_{1kP} & \\ \hat{e}_{1k2} & \hat{e}_{2k2} & \dots \hat{e}_{2kP} & \\ \vdots & \vdots & \ddots & \vdots \\ \hat{e}_{1kP} & \hat{e}_{2kP} & \dots \hat{e}_{PkP} & \end{array}\right]. \tag{33}$$

where

$$\hat{e}_{qkr} = \frac{\langle \Psi_k \Psi_r, \Psi_q \rangle}{\langle \Psi_q^2 \rangle} \tag{34}$$

#### 3.2.2 Nonlinear Part

Consider the nonlinear part of Eq. (18), that is, $\dot{\boldsymbol{x}} = \boldsymbol{h}$. We will first assume that $\boldsymbol{h}$ has a polynomial form in $\boldsymbol{x}$ (Fisher and Bhattacharya (2006)).

$$h_i(\boldsymbol{x}, \boldsymbol{\xi}) = \sum_{j=1}^{s} \eta_j(\boldsymbol{\xi}) \boldsymbol{x}^{\boldsymbol{\beta}_j}(t, \boldsymbol{\xi}) \tag{35}$$

where $\eta_j \in \mathbb{R}$ are uncertain coefficients of the polynomial of $\boldsymbol{x}$, which has $s$ terms, and $\boldsymbol{\beta}_j \in \mathbb{R}^n$, whose elements are non-negative integers, is a vector containing the order of each term in the monomial. We may represent $\eta_j(t, \boldsymbol{\xi})$ in gPC expansion as:

$$\eta_j(\boldsymbol{\xi}) \approx \sum_{k=0}^{P} \eta_{j,k} \Psi_k(\boldsymbol{\xi}). \tag{36}$$

Similar to $a_{ij,k}$ and $b_{ij,k}$, the coefficients $\eta_{j,k}$ are obtained through the projection onto $\{\Psi_q\}_{q=0}^{P}$

$$\eta_{j,k} = \frac{\langle \eta_j(\boldsymbol{\xi}), \Psi_k(\boldsymbol{\xi}) \rangle}{\langle \Psi_k^2(\boldsymbol{\xi}) \rangle}. \tag{37}$$

The substitution of the expansions for $x_i$ and $\eta_j$, Eq. (19) and (37) respectively, in Eq. (36) and subsequent Galerkin projection yields (Fisher and Bhattacharya (2006)):

$$\dot{x}_{i,q} = \sum_{j=1}^{s} \sum_{k_\eta=0}^{P} \sum_{k_{1,1}=0}^{P} \cdots \sum_{k_{n,\beta_{jn}}} \left[ \hat{e}_{q,k_\eta,k_{1,1},\dots,k_{n,\beta_{jn}}} \eta_{j,k} \prod_{r=1}^{n} \prod_{c=1}^{\beta_{jn}} x_{r,k_c} \right] \tag{38}$$

where

$$\hat{e}_{q,k_\eta,k_{1,1},\ldots,k_{n,\beta_{jn}}} = \frac{\langle \Psi_k \cdots \Psi_{k_{n,\beta_{jn}}}, \Psi_q \rangle}{\langle \Psi_q^2 \rangle}. \tag{39}$$

The inner products present in both Eq. (34) and (39) can be computed numerically. Equation (38) may be rewritten in a more compact form as

$$\dot{\boldsymbol{\mathcal{X}}} = \boldsymbol{\mathcal{H}} = \sum_{j=1}^{\hat{s}} \hat{\eta}_j \boldsymbol{\mathcal{X}}^{\hat{\boldsymbol{\beta}}_j} \tag{40}$$

where $\hat{\eta}_j$ represents the coefficients of polynomials of $\boldsymbol{\mathcal{X}}$, which has $\hat{s}$ terms, and the vector $\hat{\boldsymbol{\beta}}_j$ contains the order of each monomial.

A possible approach to representing non-polynomial functions is to expand them in Taylor series around the mean of the argument. For instance, consider the case where $h_i(\boldsymbol{x}, \boldsymbol{\xi})$ is a non-polynomial function of the single variable $x_j(\boldsymbol{\xi})$. The Taylor series expansion around the mean of $h_i$, that is, the first term of the gPC expansion according to Eq. (16), gives:

$$h_i(x_j(\boldsymbol{\xi})) \approx \sum_{p=0}^{N} \frac{h_i^{(p)}(x_{j,0})}{p!} \left( \sum_{k=0}^{P} x_{j,k} \Psi_k(\boldsymbol{\xi}) \right)^p. \tag{41}$$

Putting together the derivations presented in Sections 3.2.1 and 3.2.2, especially Eq. (28) and (40), we can write the augmented system of $n(P+1)$ deterministic ordinary differential equations for the modes strengths of the gPC expansion of the original stochastic dynamical system:

$$\dot{\boldsymbol{\mathcal{X}}} = \boldsymbol{\mathcal{A}}\boldsymbol{\mathcal{X}} + \boldsymbol{\mathcal{H}} + \boldsymbol{\mathcal{B}}\boldsymbol{\mathcal{U}} \qquad \boldsymbol{\mathcal{X}}(t_0) = \boldsymbol{\mathcal{X}}_0 \tag{42}$$

Note that this intrusive approach increased the dimension of the system by a factor equal to the order of the gPC expansion. On the other hand, the behavior of the dynamical system is now represented in a deterministic framework.

## 4. LINEAR FEEDBACK CONTROL DESIGN

Here we want to design a control system that drives the trajectories from a certain initial condition to the origin, i.e. $\boldsymbol{x}(t_f) = 0$. We formulate an optimal control problem that, given the nonlinear dynamics with parametric uncertainty in Eq. (18), aims at minimizing the following LQR-like cost function:

$$\min_{\boldsymbol{u}} J = \min_{\boldsymbol{u}} E\left[ \int_{t_0}^{t_f} (l(\boldsymbol{x}) + \boldsymbol{u}^T \boldsymbol{R} \boldsymbol{u}) \right] \tag{43}$$

where

$$l(\boldsymbol{x}) = \boldsymbol{x}^T \boldsymbol{Q} \boldsymbol{x} + N(\boldsymbol{x}), \tag{44}$$

$\boldsymbol{Q} \in \mathbb{R}^{n \times n}$ is a real symmetric and positive definite matrix and $\boldsymbol{R} \in \mathbb{R}^{m \times m}$ is a real positive definite matrix. $N(\boldsymbol{x})$ is a term that will be chosen later to account for the nonlinearities of the model.The stochastic dynamical system can be represented as in Eq. (42). Likewise note that we can write the functional in Eq. (43) in the gPC framework, just as presented in Section 1..Using the orthogonal polynomials property, one can show that (Fisher and Bhattacharya (2009)):

$$E[\boldsymbol{x}^T \boldsymbol{Q} \boldsymbol{x}] = \boldsymbol{\mathcal{X}}^T \widetilde{\boldsymbol{Q}} \boldsymbol{\mathcal{X}} \tag{45}$$

$$E[\boldsymbol{u}^T \boldsymbol{R} \boldsymbol{u}] = \boldsymbol{\mathcal{U}}^T \widetilde{\boldsymbol{R}} \boldsymbol{\mathcal{U}} \tag{46}$$

where $\widetilde{\boldsymbol{Q}} \triangleq \boldsymbol{Q} \otimes \boldsymbol{W}$, $\widetilde{\boldsymbol{R}} \triangleq \boldsymbol{R} \otimes \boldsymbol{W}$ and $\boldsymbol{W} \in \mathbb{R}^{(P+1)\times(P+1)}$ is a matrix whose elements are $\{\boldsymbol{W}\}_{ij} = \langle \Psi_i(\boldsymbol{\xi}), \Psi_j(\boldsymbol{\xi}) \rangle$. In general, the expectation of $N(\boldsymbol{x})$ can be written as a function of the gPC coefficients for $\boldsymbol{x}$:

$$E[N(\boldsymbol{x})] = \mathcal{N}(\boldsymbol{\mathcal{X}}) \tag{47}$$

Hence the cost function in Eq. (43) can be represented in a deterministic form as:

$$\min_{\boldsymbol{\mathcal{U}}} \widetilde{J} = \min_{\boldsymbol{\mathcal{U}}} \int_{t_0}^{t_f} L + \boldsymbol{\mathcal{U}}^T \widetilde{\boldsymbol{R}} \boldsymbol{\mathcal{U}} \tag{48}$$

where

$$L = \boldsymbol{\mathcal{X}}^T \widetilde{\boldsymbol{Q}} \boldsymbol{\mathcal{X}} + \mathcal{N}(\boldsymbol{\mathcal{X}}) \tag{49}$$

Note that solving the optimal control problem in Eq. (43) is equivalent to solving the problem in Eq. (48). Moreover, as demonstrated in Fisher and Bhattacharya (2006); Hover and Triantafyllou (2006), the stability of the augmented system guarantees that the original system is also stable.

**Proposition 1** : Consider the augmented system presented in Eq. (42). Let us choose $\mathcal{N}(\boldsymbol{\mathcal{X}}) = -\boldsymbol{\mathcal{H}}^T\widetilde{\boldsymbol{P}}\boldsymbol{\mathcal{X}} - \boldsymbol{\mathcal{X}}^T\widetilde{\boldsymbol{P}}\boldsymbol{\mathcal{H}}$, so that

$$L = \boldsymbol{\mathcal{X}}^T\widetilde{\boldsymbol{Q}}\boldsymbol{\mathcal{X}} - \boldsymbol{\mathcal{H}}^T\widetilde{\boldsymbol{P}}\boldsymbol{\mathcal{X}} - \boldsymbol{\mathcal{X}}^T\widetilde{\boldsymbol{P}}\boldsymbol{\mathcal{H}} \tag{50}$$

The optimal control law that transfers the dynamical states from a given initial condition to the origin while minimizing the cost function in Eq. (48), as long as $L$ is positive definite, has the form

$$\boldsymbol{\mathcal{U}} = -\widetilde{\boldsymbol{R}}^{-1}\boldsymbol{\mathcal{B}}^T\widetilde{\boldsymbol{P}}\boldsymbol{\mathcal{X}} \tag{51}$$

where $\widetilde{\boldsymbol{P}}$ is the solution of the algebraic Riccati equation

$$-\dot{\widetilde{\boldsymbol{P}}} = \widetilde{\boldsymbol{P}}\boldsymbol{\mathcal{A}} + \boldsymbol{\mathcal{A}}^T\widetilde{\boldsymbol{P}} - \widetilde{\boldsymbol{P}}\boldsymbol{\mathcal{B}}\widetilde{\boldsymbol{R}}^{-1}\boldsymbol{\mathcal{B}}^T\widetilde{\boldsymbol{P}} + \widetilde{\boldsymbol{Q}} \qquad \widetilde{\boldsymbol{P}}(t_f) = \mathbf{0} \tag{52}$$

Additionally, for $t \to \infty$, the controlled system is locally asymptotically stable in the neighborhood $\Gamma_0 \subset \Gamma, \Gamma \subset \mathbb{R}^{n(P+1)}$, of the origin if $\boldsymbol{\mathcal{X}}_0 \in \Gamma_0$. If $\Gamma = \mathbb{R}^{n(P+1)}$, then the controlled system is globally asymptotically stable.

**Proof** : See Pereira *et al.* (2016) (to appear).

## 5. NUMERICAL SIMULATIONS

In this section we show some numerical simulations of the proposed control strategy applied to the rotation dynamics of the MAV presented in Section 2. This paper makes use of the AR Drone 2 parameters in order to emulate a real plataform. The moments of inertia of the vehicle are: $J_x = 2.238 \times 10^{-3}$ kg m$^2$, $J_y = 2.986 \times 10^{-3}$ kg m$^2$ and $J_z = 4.804 \times 10^{-3}$ kg m$^2$. In the first batch of simulations, it was considered an uncertainty in the moments of inertia of $\pm 50\%$ around the nominal values. Figure 2 shows the controlled trajectories. We also show for sake of comparison the Monte Carlo based designs. We see a good agreement between the methods. Moreover, the trajectories reach the target value and, as can be seen in Fig. 3, the controlled system is asymptotically stable since $L$ is positive definite. The gain matrices were:

$$\mathbf{Q} = \begin{bmatrix} 1 & 0 & 0 & 0 & 0 & 0 \\ 0 & 1 & 0 & 0 & 0 & 0 \\ 0 & 0 & 1 & 0 & 0 & 0 \\ 0 & 0 & 0 & 1 & 0 & 0 \\ 0 & 0 & 0 & 0 & 1 & 0 \\ 0 & 0 & 0 & 0 & 0 & 1 \end{bmatrix} \qquad \mathbf{R} = \begin{bmatrix} 1000 & 0 & 0 \\ 0 & 1000 & 0 \\ 0 & 0 & 1000 \end{bmatrix} \tag{53}$$

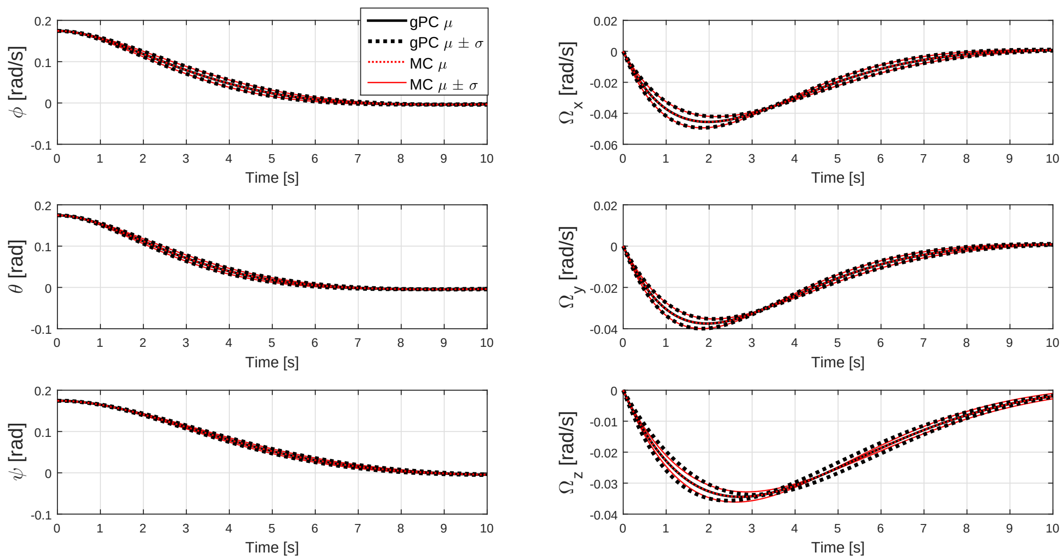


Figure 2: **Trajectory for the controlled MAV. In black, generalized polynomial chaos (gPC) based design. In red, Monte Carlo (MC) based design.**

In the second batch of simulations, it was considered that the MAV was subjected to a external disturbance in $\Omega_x$ of the form

$$w = \frac{(0.8 + 0.5\xi)9.81}{2}\left[1 - \cos\left(\frac{\pi t}{5}\right)\right]\frac{e^{-0.04t}}{t^2+1} \tag{54}$$

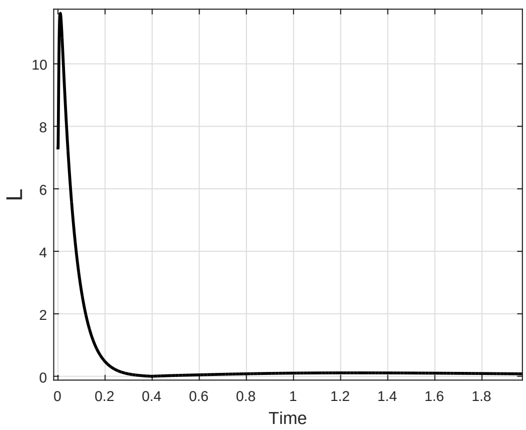


Figure 3: **Positive definite function L**

where $\xi$ $N(0,1)$. Such disturbance is an adaptation of the U.S. Military Specification MIL-F-8785C for wind gusts. Figure 4 shows the trajectories of the controlled vehicle. The gain matrices were:

$$\mathbf{Q} = \begin{bmatrix} 80 & 0 & 0 & 0 & 0 & 0 \\ 0 & 80 & 0 & 0 & 0 & 0 \\ 0 & 0 & 80 & 0 & 0 & 0 \\ 0 & 0 & 0 & 1 & 0 & 0 \\ 0 & 0 & 0 & 0 & 1 & 0 \\ 0 & 0 & 0 & 0 & 0 & 1 \end{bmatrix} \qquad \mathbf{R} = \begin{bmatrix} 1 & 0 & 0 \\ 0 & 1 & 0 \\ 0 & 0 & 1 \end{bmatrix} \tag{55}$$

Again, we plot the Monte Carlo based designs. Both methods provides similar results in the statistical standpoint. The control law was able to successfully drive the trajectories to the equilibrium state.

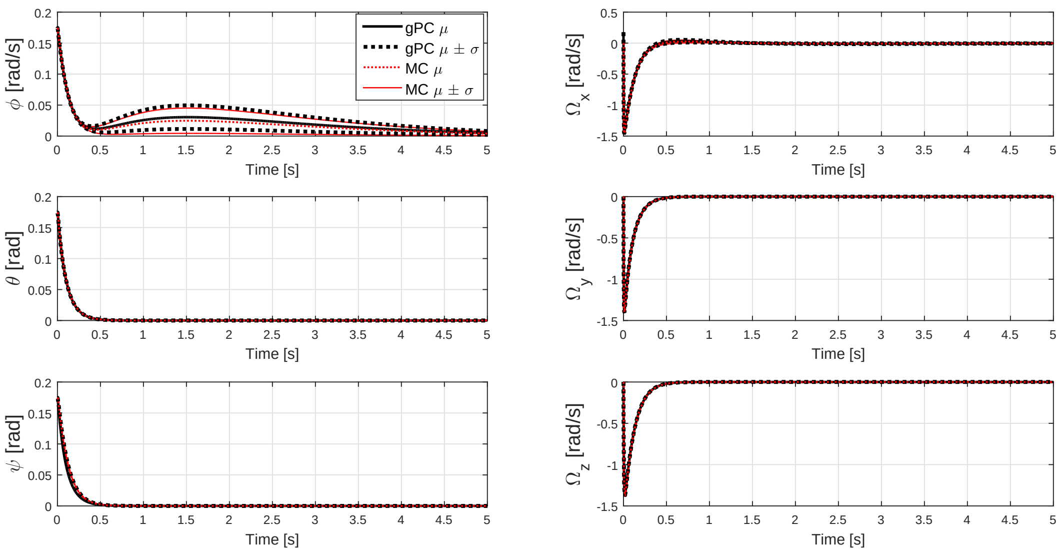


Figure 4: **Trajectory for the controlled MAV subjected to disturbance. In black, generalized polynomial chaos (gPC) based design. In red, Monte Carlo (MC) based design.**

## 6. CONCLUSIONS

In this paper we have presented an optimal linear feedback control design method for the attitude control nonlinear MAV model with stochastic uncertain parameters. We also analyzed the performance of the controlled vehicle subjected to random disturbances. Using the generalized polynomial chaos expansions, parameterized by random variables with known distribution, the stochastic differential equation that describes the dynamics of the system is transformed into an augmented system of deterministic differential equations for the mode strengths of the spectral decomposition. The feedback control design, formulated under the optimal control theory, is then performed in a deterministic framework. Numerical simulations shows that the control laws are effective and the results are consistent with the conventional Monte Carlo based analysis in the statistical viewpoint. As future work, we consider applying the proposed control strategy to a complete MAV model, for both rotational and translational dynamics, in a uncertain environment. Moreover, we consider study the implementation of such control strategy in a real vehicle, which may require estimation algorithms.

## 7. ACKNOWLEDGEMENTS

This research work is supported by the Conselho Nacional de Desenvolvimento Científico e Tecnológico (CNPQ, Brazil), which has granted a scholarship to the first author, and by the Coordenação de Aperfeiçoamento de Pessoal de Nivel Superior (CAPES), which has granted a scholarship to the first and second co-authors.

## 8. REFERENCES

Askey, R. and Wilson, J., 1985. "Some basic hypergeometric polynomials that generalize jacobi polynomials". *Memoirs of the American Mathematical Society*, Vol. 319.

Bialy, B.J., Klotz, J., Brink, K. and Dixon, W.E., 2013. "Lyapunov-based robust adaptive control of a quadrotor uav in the presence of modeling uncertainties".

Bouabdallah, S., Noth, A. and Siegwart, R., 2004. "Pid vs lq control techniques applied to an indoor micro quadrotor". In *Proceedings of the IEEE/RSJ International Conference on Intelligent Robots and Systems*. New Orleans, pp. 2451–2456.

Branicki, M. and Majda, A.J., 2012. "Fundamental limitations of polynomial chaos for uncertainty quantification on systems with intermittent instabilities". *Communications in Mathematical Sciences*, Vol. 11(1), pp. 55–103.

Cameron, R.H. and Martin, W.T., 1947. "The orthogonal development of non-linear functionals in series of fourier-hermite functionals". *The Annals of Mathematics*, Vol. 48(2), pp. 385–392.

Cheviron, T., Hamel, T., Mahony, R. and Baldwin, G., 2007. "Robust nonlinear fusion of inertial and visual data for position, velocity and attitude estimation of uav". In *Proceedings of the IEEE International Conference on Robotics and Automation*. Roma, pp. 2010–2016.

Fisher, J. and Bhattacharya, R., 2006. "Application of polynomial chaos in stability and control". *Automatica*, Vol. 42, pp. 789–795.

Fisher, J. and Bhattacharya, R., 2008. "On stochastic lqr design and polynomial chaos". In *Proceedings of the American Control Conference*. ACC, Seattle, USA.

Fisher, J. and Bhattacharya, R., 2009. "Linear quadratic regulation of systems with stochastic parameter uncertainties". *Automatica*, Vol. 45(12), pp. 2831–2841.

Hover, F.S. and Triantafyllou, M.S., 2006. "Application of polynomial chaos in stability and control". *Automatica*, Vol. 42, pp. 789–795.

Kada, B. and Ghazzawi, Y., 2011. "Robust pid controller design fo".

Pereira, M.F.V., Balthazar, J.M., Santos, D.A., Tusset, A.M., Castro, D.F. and Prado, I.A.A., 2016. "A note on polynomial chaos expansions for designing a linear feedback control for nonlinear systems". *Nonlinear Dynamics (submitted)*.

Prabhakar, A., Fisher, J. and Bhattacharya, R., 2010. "Polynomial chaos-based analysis of probabilistic uncertainty in hypersonic flight dynamics". *Journal of Guidance and Control*, Vol. 33(1), pp. 222–234.

Prado, I.A.A. and Santos, D.A., 2014. "A safe position tracking strategy for multirotor helicopters". In *22nd Mediterranean Conference on Control and Automation*.

Raffo, G.V., Ortega, M.G. and Rubio, F.R., 2010. "An integral predictive/nonlinear $\mathcal{H}_\infty$ control structure for a quadrotor helicopter." *Automatica*, Vol. 46, No. 1, pp. 29–39.

Rafikov, M. and Balthazar, J.M., 2008. "On control and synchronization in chaotic and hyperchaotic systems via linear feedback control". *Communications in Nonlinear Science and Numerical Simulation*, Vol. 12, pp. 1246–1255.

Rafikov, M., Balthazar, J.M. and Tusset, A.M., 2008. "An optimal linear design for nonlinear systems". *Journal of the Brazilian Society of Mechanical Sciences & Engineering*, Vol. 30(4), pp. 279–284.

Santos, D.A., Saotome, O. and Cela, A., 2013. "Trajectory control of multirotor helicopters with thrust vector constraints". In *21st Mediterranean Conference on Control and Automation*. Chania, pp. 375–379.

Saripalli, S., Montgomery, J.F. and Sukhatme, G.S., 2003. "Visually-guided landing of an unmanned aerial vehicle". *IEEE Transactions on Robotics and Automation*, Vol. 10, No. 3, pp. 371–381.

Wiener, N., 1938. "The homogeneous chaos". *American Journal of Mathematics*, Vol. 60(4), pp. 897–936.

Xiu, D. and Karniadakis, G.E., 2002. "The wiener-askey polynomial chaos for stochastic differential equations". *SIAM Journal on Scientific Computing*, Vol. 24(2), p. 619–644.

Xiu, D. and Karniadakis, G.E., 2003. "Modeling uncertainty in flow simulations via generalized polynomial chaos". *Journal of Computational Physics*, Vol. 187(1), pp. 137–167.

## 9. RESPONSIBILITY NOTICE

The authors are the only responsible for the printed material included in this paper.